FULL PAPER

Dalton
www.rsc.org/dalton

Tailoring hydrophilic *N*,*N*-dialkyl-*N′*-acylthioureas suitable for Pt(II), Pd(II) and Rh(III) chloride pre-concentration from acid aqueous solutions, and their complex separation by reversed-phase HPLC †

Alpheus N. Mautjana, Jörn D. S. Miller, A. Gie, Susan A. Bourne ‡ and Klaus R. Koch *
Department of Chemistry, University of Stellenbosch, P Bag X1, Matieland, Stellenbosch, 7602, South Africa. E-mail: krk@sun.ac.za

Received 29th November 2002, Accepted 20th January 2003
First published as an Advance Article on the web 23rd April 2003

A series of new, relatively hydrophilic, *N*,*N*-dialkyl-*N′*-(2,2-dimethylpropyl)thioureas (HL^n) (n = 1, *N*,*N*-dimethyl-; n = 2, *N*-pyrrolidyl-; n = 3, *N*-piperidyl-) and their corresponding *cis*-[$M(L^n\text{-}S,O)_2$] [for M = Pt(II), Pd(II); n = 1–3] and *fac*-[$Rh(L^n\text{-}S,O)_3$] (n = 2, 3) complexes have been prepared and characterised. The crystal and molecular structures of *fac*-tris(*N*-pyrrolidyl-*N′*-(2,2-dimethylpropyl)thioureato)rhodium(III) and *cis*-bis(*N*-piperidyl-*N′*-(2,2-dimethylpropyl)-thioureato)platinum(II) are reported, as representative examples. The favourable physiochemical properties and ready formation of stable mono-isomeric *cis*-[$Pt(L^n\text{-}S,O)_2$] and *cis*-[$Pd(L^n\text{-}S,O)_2$] complexes with these ligands makes these compounds suitable for the reversed-phase high performance liquid chromatography (RP-HPLC) determination of traces of these metal ions in hydrochloric acid, following *in situ* complex formation in a homogeneous acetonitrile–hydrochloric acid phase and subsequent salt (NaCl) induced phase separation. A study of the effect of ligand structure on the separation behaviour of *cis*-[$M(L^n\text{-}S,O)_2$] of Pd(II) and Pt(II) complexes has been undertaken, showing that the nature of the ligand has a significant influence on the separation characteristics of these complexes.

The potential of use of ligands based on the *N*,*N*-dialkyl-*N′*-(acyl)aroylthiourea motif below, as selective ligands for the solvent extraction [1,2] and potential thin layer chromatographic separation of platinum group metal (PGM) ions, has previously been documented.[3–5] Moreover, a highly selective method of pre-concentration with *N*,*N*-diethyl-*N′*-benzoylthiourea followed by the ultra-trace determination of Pd(II) using electrothermal atomic absorption spectroscopy has been developed.[6]

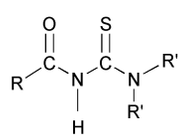

R = aroyl or alkyl; R' = alkyl groups

In the past few years, we have studied the fundamental co-ordination chemistry of mainly *N*,*N*-dialkyl-*N′*-benzoyl-thioureas toward the PGMs in some detail, with a view to understanding this co-ordination chemistry better and finding practical applications suitable for use in the PGM process industry chemistry.[7,8] These versatile ligands usually display selective, pH dependent coordination towards the PGM ions; the selectivity of coordination toward the PGMs over the first row transition metals increases significantly in acid solutions. This property makes these ligands potentially suitable for a number of practical applications such as pre-concentration and separation of, in particular, Pt(II), Pd(II) and Rh(III) ions which are refined from strongly acidic solutions in practice. Ligands derived from *N*,*N*-dialkyl-*N′*-benzoylthiourea, and their corresponding metal complexes, are unfortunately very soluble only in water-immiscible solvents such as chloroform and methylene chloride, which although advantageous for the solvent-extraction of the PGMs [2] and their thin-layer *normal*-phase chromatographic separation,[3–5] limits the practical use of these ligands and their complexes to some extent in the process chemical solutions which usually contain very high concentrations of hydrochloric acid (2–6 M). This problem is illustrated by the failure of an attempted normal-phase HPLC separation protocol based on Pt(II) and Pd(II) complexes derived from *N*,*N*-dialkyl-*N′*-benzoylthioureas, for which we found extensive on-column complex decomposition under operating pressures in the silica-based HPLC columns.[9] This problem is presumably the result of the notorious sensitivity of silica-based normal-phase columns to unavoidable traces of water and acids (notably HCl) in samples and the non-aqueous chromatographic mobile phases. Moreover the inherent acidic nature of silica-based stationary phases, which can interact strongly with metal complexes, may result in analyte decomposition and irreversible retention of highly polar analytes. We have shown previously that the presence of traces of hydrochloric acid in chloroform solution results in the facile protonation of the bound ligand in *cis*-[$Pt(L\text{-}S,O)_2$] complexes, to yield several complex species such as *cis*-[Pt(L-*S*,*O*)(HL-*S*)Cl], *cis*-[$Pt(HL\text{-}S)_2Cl_2$] and *trans*-[$Pt(HL\text{-}S)_2Cl_2$] in solution.[10,11] Such phenomena are obviously deleterious for any contemplated normal-phase chromatographic separations of *cis*-[$Pt(L\text{-}S,O)_2$] and *cis*-[$Pd(L\text{-}S,O)_2$] complexes.

As part of our ongoing interest in developing practical analytical and process-chemistry-related applications of these ligands, we wished to explore the potential *in situ* complex formation of Pt(II), Pd(II) and Rh(III) in acidic aqueous solutions using relatively *hydrophilic* ligands based on an *N*,*N*-dialkyl-*N′*-aroyl- or -acyl-thiourea motif, followed by the complex separation and quantification by means of *reversed*-phase HPLC (RP-HPLC). To our knowledge, there are no reports of the synthesis and co-ordination properties of *N*,*N*-dialkyl-*N′*-acylthioureas in the literature. We anticipated that the physicochemical properties, particularly the solubilities of *N*,*N*-dialkyl-*N′*-acylthioureas and their PGM complexes, to differ significantly from those of the *N*,*N*-dialkyl-*N′*-benzoyl-thioureas, and thus to be favourable for RP-HPLC separations in which the aqueous mobile phase could be subject to appropriate pH control, thus obviating the problems of protonation of complexes alluded to above.

We here report the synthesis of a series *N*,*N*-dialkyl-*N′*-acylthioureas, finding that a wide variety of derivatives based

† Based on the presentation given at Dalton Discussion No. 5, 10–12th April 2003, Noordwijkerhout, The Netherlands.
‡ Current address: Department of Chemistry, University of Cape Town, P Bag, Rondebosch, Cape Town, 7707, South Africa.

DOI: 10.1039/b211885h

on the RC(O)NHC(S)NR′R″ motif, with varying physico-chemical properties can readily be prepared in high yields. The co-ordination chemistry of Pt(II), Pd(II) and Rh(III) with the new ligands *N*,*N*-dimethyl-*N*′-(2,2-dimethylpropyl)thiourea (HL^1), *N*-pyrrolidyl-*N*′-(2,2-dimethylpropyl)thiourea (HL^2), and *N*-piperidyl-*N*′-(2,2-dimethylpropyl)thiourea (HL^3) is as expected,[7,8] and will only be briefly described. The general structure and numbering scheme used for these new ligands in this work is shown below.

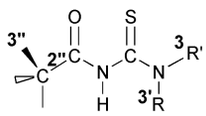

HL^1: R, R' = CH_3 ; HL^2: R,R' =  ; HL^3: R,R' = 

Moreover, we have studied the RP-HPLC separation and quantification characteristics of these new *cis*-[Pt(L^n-*S*,*O*)$_2$], *cis*-[Pd(L^n-*S*,*O*)$_2$] and *fac*-[Rh(L-*S*,*O*)$_3$] complexes, as well as some related chelates of Pd(II) and Pt(II) derived from *N*,*N*-dialkyl-*N*′-benzoylthioureas and *N*,*N*-dialkyl-*N*′-naphthoylthioureas, in an attempt to examine the influence of ligand structure on the overall separation characteristics of the *cis*-[M(L^n-*S*,*O*)$_2$] complexes, and to identify the ligand(s), with the most favourable properties for effecting Pt(II) and Pd(II) complex separations.

Experimental

Preparative methods

All ligands in this work were prepared according to a slightly modified procedure of Douglass and Dains,[12] using commercially available reagents. The 2,2-dimethylpropanoyl chloride was used without further purification, while the amines piperidine and pyrrolydine were dried over calcium hydride followed by distillation under nitrogen prior to use. Analytical grade acetone was dried over potassium carbonate and type 4 Å Linde molecular sieves, and distilled prior to use. The analytical grade potassium thiocyanate was dried in a heated vacuum pistol (110 °C) immediately before use. Care was taken throughout the synthesis to exclude moisture, and all preparations were carried out under dry nitrogen; this precaution maximises yields.

General procedure for the synthesis of *N*,*N*-dialkyl-*N*′-(2,2-dimethylpropyl)thioureas

To a solution containing 0.03 mol potassium thiocyanate in 75 cm^3 freshly distilled acetone was added drop-wise an equimolar quantity of 2,2-dimethylpropanoyl chloride (0.03 mol) in anhydrous acetone. The mixture was heated under reflux for 45 min, and cooled to room temperature under nitrogen. To this stirred reaction mixture, was added drop-wise 0.03 mol of the desired amine in 75 cm^3 acetone over 10 min, followed by heating under reflux for a further 60 min. After cooling, the mixture was poured into 75–100 cm^{3}of cold water and the acetone allowed to evaporate off in a fume-hood; this results in the precipitation of the crude product. Re-crystallisation of the dried product was from acetone–water or ethanol–chloroform mixtures; this gives good yields of colourless crystals of the ligands.

***N*,*N*-Dimethyl-*N*′-(*2*,*2*-dimethylpropanoyl)thiourea (HL^1).** (This substance was prepared as above, but the dimethylamine was used in gaseous form. Volatile dimethylamine, which was collected in a liquid-nitrogen-cooled trap was generated under nitrogen from dimethylammonium hydrochloride after cautious addition of an excess of 5 M NaOH. Approximately 0.06 mol of dried dimethylamine at room temperature was allowed to bubble into the acetone solution containing 0.03 mol 2,2-dimethylpropanoyl chloride, over 60 min; the mixture was then stirred for 2 h under a positive pressure of nitrogen without heating.)

Colourless crystals, yield 90%, m.p. 81–82 °C. Found: C, 51.3; H, 8.9; N, 15.3; S, 17.0%. $C_8H_{16}N_2OS$ requires: C, 51.0; H, 8.6; N, 14.9; S, 17.0. δ(^{13}C) (50.31 MHz, $CDCl_3$): C(3″) 27.04, C(2″)39.61, C(3′) 44.15, C(3) 42.90, C(S) 180.32, C(O) 174.36 ppm. ε(λ_{max} 218 nm) = 11 719, ε(λ_{max} 282 nm) = 15 812 dm^3 mol^{-1} cm^{-1}.

***N*-Pyrrolidyl-*N*′-(2,2-dimethylpropanoyl)thiourea (HL^2).** White crystals, 90.1% yield, m.p. 136–137 °C. Found: C, 57.0, H, 8.8; N, 13.3, S, 14.8%. $C_{10}H_{18}N_2OS$ requires: C, 57.8; H, 8.5; N, 13.1; S, 14.96. δ(^{13}C) (50.31 MHz, $CDCl_3$): C(3″) 27.16, C(2″) 39.62, C(3′) 54.43, C(3) 52.52, C(4′) 26.16, C(4) 24.59, C(S) 176.66, C(O) 174.38 ppm. ε(λ_{max} 216 nm) = 13 399, ε(λ_{max} 276 nm) = 14 792 dm^3 mol^{-1} cm^{-1}.

***N*-Piperidyl-*N*′-(2,2-dimethylpropanoyl)thiourea (HL^3).** White crystals, 96% yield, m.p. 90–92 °C. Found: C, 58.2; H, 9.1; N 12.3; S, 13.9%. $C_{11}H_{20}N_2OS$ requires: C, 57.8; H, 8.8; N, 12.3; S, 14.04. δ(^{13}C) (50.31 MHz, $CDCl_3$): C(3″) 27.06, C(2″) 39.64, C(3′) 52.87, C(3) 52.87, C(4′) 26.01, C(4) 25.19, C(5) 23.83, C(S) 178.49, C(O) 174.08 ppm. ε(λ_{max} 216 nm) = 13 737, ε(λ_{max} 276 nm) = 15 373 dm^3 mol^{-1} cm^{-1}.

Synthesis of platinum(II), palladium(II) and rhodium(III) complexes

A solution containing 0.5 mmol quantities of K_2PdCl_4 (163.2 mg) or K_2PtCl_4 (207.6 mg, prepared from 15 cm^3 of water and 10 cm^3 acetonitrile), was added drop-wise to a constantly stirred ligand solution, made from 1 mmol equivalent of the *N*-substituted-*N*′-(2,2-dimethylpropanoyl)thiourea ligand dissolved in 15 cm^3 acetonitrile and 10 cm^3 of water containing 165 mg (2 mmol) of sodium acetate. The final solvent composition was 50(v/v)% water–acetonitrile. The mixture was stirred at room temperature for 2 h, after which 50–100 cm^3 of water was added. The yellow/orange precipitate which formed on standing at 4 °C overnight was isolated by centrifugation, washed twice with small portions of ice-cold water, and dried under vacuum at 60 °C.

Rhodium(III) complexes, Rh[L-(*S*,*O*)]$_3$, were similarly prepared from dry, commercially available $RhCl_3$·$3H_2O$, excepting that metal:ligand ratios of 1:3 in 50(v/v)% water–acetonitrile mixtures with 3 equiv. of sodium acetate were used, and the resulting reaction mixture was heated under reflux for *ca.* 20 h.

Bis[*N*,*N*-dimethyl-*N*′-(2,2-dimethylpropanoyl)thioureato]-palladium(II). Dark orange crystals, 99% yield, m.p. 196–198 °C. Found: C, 40.1; H, 6.4; N, 11.7; S, 13.4%. $C_{16}H_{30}N_4O_2PdS_2$ requires: C, 40.0; H, 6.3; N, 11.6; S, 13.3. δ(^{13}C) (50.31 MHz, $CDCl_3$): C(3″) 28.57, C(2″) 41.90, C(3′) 41.76, C(3) 40.61, C(S) 171.93, C(O) 185.58 ppm. ε(λ_{max} 216 nm) = 44 511, ε(λ_{max} 276 nm) = 61 702 dm^3 mol^{-1} cm^{-1}.

Bis[*N*,*N*-pyrrolidyl-*N*′-(2,2-dimethylpropanoyl)thioureato]-palladium(II). Dark orange crystals, 99% yield, m.p. 212–215 °C. Found: C, 45.0; H, 6.4; N, 10.3; S, 11.9%. $C_{20}H_{34}N_4O_2PdS_2$ requires: C, 45.1; H, 6.4; N, 10.5; S, 12.0. δ(^{13}C) (50.31 MHz, $CDCl_3$): C(3″) 28.57, C(2″) 41.76, C(3′) 50.37, C(3) 50.30, C(4′) 25.43, C(4) 24.77, C(S) 168.38, C(O) 185.20 ppm. ε(λ_{max} 216 nm) = 41 140, ε(λ_{max} 276 nm) = 51 861 dm^3 mol^{-1} cm^{-1}.

Bis[*N*-piperidyl-*N*′-(2,2-dimethylpropanoyl)thioureato]-palladium(II). Dark orange crystals, 91% yield, m.p. 192–194 °C. Found: C, 47.2; H, 6.9; N, 10.1; S, 11.3%. $C_{22}H_{38}N_4O_2PdS_2$ requires: C, 47.1; H, 6.8; N, 10.0; S, 11.4. δ(^{13}C) (50.31 MHz, $CDCl_3$): C(3″) 28.54, C(2″) 41.87, C(3′) 50.82, C(3) 48.24, C(4′)

26.04, C(4) 25.87, C(5) 24.54, C(S) 170.64, C(O) 185.93 ppm. $\varepsilon(\lambda_{max}$ 218 nm) = 37209, $\varepsilon(\lambda_{max}$ 280 nm) = 60483 dm^3 mol^{-1} cm^{-1}.

Bis[*N*,*N*-dimethyl-*N*′-(2,2-dimethylpropanoyl)thioureato]-platinum(II). Yellow crystals, 100% yield, m.p. 210–213 °C. Found: C, 34.0; H, 5.4; N, 9.8; S, 11.5%. $C_{16}H_{30}N_4O_2PtS_2$ requires: C, 33.7; H, 5.3; N, 9.8; S, 11.2. δ(^{13}C) (50.31 MHz, $CDCl_3$): C(3″) 28.22, C(2″) 42.26, C(3′) 41.42, C(3) 40.42, C(S) 167.83, C(O) 183.26 ppm. $\varepsilon(\lambda_{max}$ 206 nm) = 53265, $\varepsilon(\lambda_{max}$ 254 nm) = 34879, $\varepsilon(\lambda_{max}$ 306 nm) = 24729 dm^3 mol^{-1} cm^{-1}.

Bis[*N*-pyrrolidyl-*N*′-(2,2-dimethylpropanoyl)thioureato]-platinum(II). Yellow crystals, 73% yield, m.p. 214–218 °C. Found: C, 38.5; H, 5.5; N, 9.0; S, 10.2%. $C_{20}H_{34}N_4O_2PtS_2$ requires: C, 38.6; H, 5.5; N, 9.0; S, 10.3. δ(^{13}C) (50.31 MHz, $CDCl_3$): C(3″) 28.36, C(2″) 42.12, C(3′) 50.22, C(3) 49.99, C(4′) 25.29, C(4) 24.71, C(S) 164.31, C(O) 182.92 ppm. $\varepsilon(\lambda_{max}$ 206 nm) = 58449, $\varepsilon(\lambda_{max}$ 258 nm) = 43894, $\varepsilon(\lambda_{max}$ 306 nm) = 29476 dm^3 mol^{-1} cm^{-1}.

Bis[*N*-piperidyl-*N*′-(2,2-dimethylpropanoyl)thioureato]-platinum(II). Yellow crystals, 78% yield, m.p. 206–210 °C. Found: C, 40.9; H, 5.9; N, 8.7; S, 10.0%. $C_{22}H_{38}N_4O_2PtS_2$ requires: C, 40.7; H, 5.9; N, 8.6; S, 9.9. δ(^{13}C) (50.31 MHz, $CDCl_3$): C(3″) 28.27, C(2″) 42.22, C(3′) 47.97, C(3) 50.35, C(4′) 24.49, C(4) 25.79, C(5) 25.79, C(S) 166.60, C(O) 183.59 ppm. $\varepsilon(\lambda_{max}$ 208 nm) = 55017, $\varepsilon(\lambda_{max}$ 260 nm) = 38015, $\varepsilon(\lambda_{max}$ 312 nm) = 27173 dm^3 mol^{-1} cm^{-1}.

Tris[*N*-pyrrolidyl-*N*′-(2,2-dimethylpropanoyl)thioureato]-rhodium(III). Orange crystals, 75% yield, m.p. 251–254 °C. Found: C, 43.7; H, 6.2; N, 10.0; S, 11.2%. $RhC_{30}H_{51}N_6O_3S_3\cdot CHCl_3$ requires: C, 43.18; H, 6.08; N, 9.74; S, 11.16. δ(^{13}C) (50.31 MHz, $CDCl_3$): C(3″) 28.89, C(2″) 42.41, C(3′) 51.16, C(3) 49.75, C(4′) 25.67, C(4) 25.00, C(S) 170.91, C(O) 186.47 ppm. $\varepsilon(\lambda_{max}$ 220 nm) = 39146, $\varepsilon(\lambda_{max}$ 264 nm) = 41429 dm^3 mol^{-1} cm^{-1}.

Tris-[*N*-piperidyl-*N*′-(2,2-dimethylpropanoyl)thioureato]-rhodium(III). Orange crystals, 72% yield, m.p. 210–212 °C. Found: C, 45.9; H, 6.6; N, 9.1; S, 10.6%. $RhC_{33}H_{57}N_6O_3S_3\cdot CHCl_3$ requires: C, 45.06; H, 6.45; N, 9.27; S, 10.61. δ(^{13}C) (50.31 MHz, $CDCl_3$): C(3″) 28.52, C(2″) 42.12, C(3′) 47.61, C(3) 49.61, C(4′) 25.87, C(4) 25.87, C(5) 24.60, C(S) 172.85, C(O) 186.77 ppm. $\varepsilon(\lambda_{max}$ 222 nm) = 39843, $\varepsilon(\lambda_{max}$ 264 nm) = 41988 dm^3 mol^{-1} cm^{-1}.

NMR spectroscopy

Conventional ^{1}H and ^{13}C NMR spectra of the ligands and complexes were recorded at low field (4.7 Tesla) at 25 °C in $CDCl_3$ solutions using a Varian VXR 200 spectrometer, operating at 199.98 and 50.31 MHz, respectively. All other spectra were acquired on a Varian Unity Spectrometer, operating at 499.84 MHz for ^{1}H, 125.67 MHz for ^{13}C and 107.16 MHz for ^{195}Pt. For the experiments involving direct ^{195}Pt observation, the spectrometer was equipped with a 5 mm broad-band probe. All ^{195}Pt NMR shifts (at 30 °C) are reported (±2 ppm) relative to the generally used external reference: 500 mg cm^{-3} H_2PtCl_6 in 30% (v/v) D_2O/1 M HCl.[13]

X-Ray diffraction

Data were collected using a Nonius Kappa CCD with 1.5 kW graphite monochromatic Mo radiation. The strategy for the data collection was evaluated using the Collect Software.[14] The detector-to-crystal distance was 45 mm. Exposure times of 2 × 45 s per frame and scan widths of 2.0° were used throughout the data collection. The four sets of data were combined using Denzo-SMN.[15] Scaling was suppressed in order that absorption corrections could be applied. The structure was solved and refined using X-SEED[16] and SHELX97.[17] All non-hydrogen atoms for *cis*-[Pt(L^3-*S*,*O*)$_2$] were refined anisotropically, while in the case of *fac*-[Rh(L^2-*S*,*O*)$_3$]·$CHCl_3$, the final model included anisotropic refinement of non-hydrogen atoms, excepting the carbon atoms of the 2,2-dimethylpropyl group, as these exhibited considerable thermal motion. For both structures, hydrogen atoms were placed in calculated positions and included in the model during final stages of the refinement. Pertinent crystal data are given in Table 1.

CCDC reference numbers 198812 and 198813.

See http://www.rsc.org/suppdata/dt/b2/b211885h/ for crystallographic data in CIF or other electronic format.

HPLC instrumentation, analysis and conditions

Chromatographic analyses were carried out with one of two HPLC systems. Initial data were collected using a Spectra-Series HPLC system equipped with a P200 pump, a manual injector, a LUNA-ODS (C_{18}), 5 μm particle, 150 × 4.6 mm column, a UV150 detector, and a data system using the Delta 5.0 chromatography integration software. Alternatively, a Waters 2690 'Alliance' fully automatic HPLC system equipped with automatic sample injection system and a Waters 996 photodiode array detector, using a 4.6 × 150 mm, 5 μm, Zorbax Eclipse XDB-C18 column. Only de-ionized water and HPLC-grade acetonitrile were used to make up the mobile phases. Acetate buffer of pH ≈ 6 was prepared by mixing exactly 25 cm^3 of 0.1 mol dm^{-3} acetic acid with 475 cm^3 of 0.1 mol dm^{-3} sodium acetate solution. All eluents were finally filtered through a 0.45 μm (Microsep) nitrocellulose membrane and degassed by bubbling helium gas through eluent reservoirs for at least 1 h prior to use. The column was conditioned with an acetonitrile–aqueous buffer mixture [90:10 (%v/v)], usually at 1 cm^3 min^{-1} for 15–30 min before commencing with sample (20 μl) injections.

Results and discussion

Synthesis and structure of *cis*-[Pt(L^n-*S*,*O*)$_2$], *cis*-[Pd(L^n-*S*,*O*)$_2$] and *fac*-[Rh(L^n-*S*,*O*)$_3$]

Treatment of solutions of the ligands HL^n (n = 1–3) in acetonitrile–water (1:1, v/v) containing 2 equiv. sodium acetate with the required quantities of K_2PtCl_4, K_2PdCl_4 or $RhCl_3\cdot 3H_2O$ in the same solvent, leads to high yields of complexes of the type *cis*-[M(L^n-*S*,*O*)$_2$] [for M = Pt(II) or Pd(II), n = 1–3], and [M(L^n-*S*,*O*)$_3$] [for M = Rh(III), n = 2, 3]. These complexes are soluble in a number of polar solvents and slightly soluble in acetonitrile–water mixtures. While the ^{1}H NMR spectra of these complexes in $CDCl_3$ are deceptively simple, the ^{13}C NMR spectra (recorded at 4.7 Tesla, 50.3 MHz)§ are particularly informative as a result of well resolved long range ^nJ(^{195}Pt–^{13}C) and ^nJ(^{103}Rh–^{13}C) coupling patterns. These spectra show that only a single isomer for each of the metal complexes {*cis*-[Pt(L^n-*S*,*O*)$_2$], *cis*-[Pd(L^n-*S*,*O*)$_2$] and *fac*-[Rh(L^n-*S*,*O*)$_3$]} is formed, consistent with published data of the corresponding *N*,*N*-dialkyl-*N*′-benzoylthiourea complexes of Pt(II) and Pd(II).[19] The ^{195}Pt NMR chemical shifts of the [Pt(L^n-*S*,*O*)$_2$] complexes fall in the region −2700 to −2770 ppm, typical of the *cis* configuration,[19] the *cis* configuration of the representative crystal structure of *cis*-[Pt(L^3-*S*,*O*)$_2$] being confirmed below. Table 2 lists some important ^{13}C and ^{195}Pt NMR data characteristic of these *cis*-[Pt(L^n-*S*,*O*)$_2$], *cis*-[Pd(L^n-*S*,*O*)$_2$] and *fac*-[Rh(L^n-*S*,*O*)$_3$] complexes. The table also shows δ(^{195}Pt) shifts, ^nJ(^{195}Pt–^{13}C) and ^3J(^{103}Rh–^{13}C) coupling constants as well as interesting chemical

§ ^{13}C NMR spectra were recorded at 4.7 Tesla to avoid the CAS[18] broadening for ^{195}Pt isotopomers at higher magnetic fields. For ^{13}C spectra recorded at 100.6 MHz (9.6 Tesla), no ^{195}Pt satellites are visible in the spectra of the [Pt(L^n-*S*,*O*)$_2$] complexes.

Table 1 Crystal data for *cis*-bis[*N*-piperidyl-*N′*-(2,2-dimethylpropyl)thioureato]platinum(II) and of *fac*-tris[*N*-pyrrolidyl-*N′*-(2,2-dimethylpropyl)-thioureato]rhodium(III)

Complex	*cis*-[Pt(L^3-*S*,*O*)$_2$]	*fac*-[Rh(L^2-*S*,*O*)$_3$]·$CHCl_3$
Empirical formula	$C_{22}H_{38}N_4O_2PtS_2$	$C_{30}H_{51}N_6O_3RhS_3$·$CHCl_3$
Formula weight	649.77	862.23
T/K	198(2)	293(2)
Wavelength/Å	0.71073	0.71073
Crystal system	Monoclinic	Triclinic
Space group	$P2_1/c$	$P\bar{1}$
a/Å	9.951(2)	10.697(4)
b/Å	15.235(3)	13.454(6)
c/Å	18.358(4)	14.432(6)
α/°	90	84.77(3)
β/°	105.20(3)	89.81(3)
γ/°	90	78.88(3)
V/Å^3	2685.7(9)	2029.3(15)
Z	4	2
D_c/Mg m^{-3}	1.607	1.411
Absorption coefficient/mm^{-1}	5.404	0.811
F(000)	1296	896
Crystal size/mm	0.21 × 0.40 × 0.25	0.30 × 0.35 × 0.40
θ Range for data collection/°	2.7–27	1.42–24.98
Index ranges	$-10 \leqslant h \leqslant 12$ $-13 \leqslant k \leqslant 19$ $-23 \leqslant l \leqslant 23$	$-12 \leqslant h \leqslant 12$ $0 \leqslant k \leqslant 15$ $-16 \leqslant l \leqslant 17$
Reflections collected	21 204	7123
Independent reflections	5902 (R_{int} = 0.0566)	7123 (R_{int} = 0.0006)
Completeness to θ(%)	97 (to θ 27°)	99.8 (to θ 24.98°)
Refinement method	Full-matrix least-squares on F^2	Full-matrix least-squares on F^2
Data/restraints/parameters	5902/0/281	7123/0/379
Goodness-of-fit on F^2	1.033	1.040
Final R indices [$I > 2\sigma(I)$]	R_1 = 0.0314, wR_2 = 0.0788	R_1 = 0.0773, wR_2 = 0.2124
R indices (all data)	R_1 = 0.0378, wR_2 = 0.0827	R_1 = 0.0954, wR_2 = 0.2259
Largest diff. peak and hole/e Å^{-3}	1.779 and −1.757	2.293 and −2.611

Table 2 Selected ^{195}Pt and ^{13}C NMR data for the *cis*-[M(L^n-*S*,*O*)$_2$] [for M = Pt(II), Pd(II), n = 1–3] and *fac*-[Rh(L^n-*S*,*O*)$_3$] (n = 2, 3) complexes studied here; $^nJ(^{195}Pt–^{13}C)$ and $^nJ(^{103}Rh–^{13}C)$ are the resolved coupling constants, while $\Delta[\delta^{13}C(S)]$/ppm and $\Delta[\delta^{13}C(O)]$/ppm are the chemical shift displacements induced in the $\delta^{13}C(S)$ and $^{13}C(O)$ on complex formation, defined as $\Delta = (\delta^{13}C_{complex} - \delta^{13}C_{ligand})$

Complex	$\delta(^{195}Pt)$/ppm [a]	$^2J[^{195}Pt–^{13}C(S)]$/Hz	$^3J[^{195}Pt–^{13}C(2'')]$/Hz	$^4J[^{195}Pt–^{13}C(3')]$/Hz	$\Delta[\delta^{13}C(S)]$/ppm [b]	$\Delta[\delta^{13}C(O)]$/ppm [b]
cis-[Pt(L^1-*S*,*O*)$_2$]	−2745	46	21	30	−12.5	8.9
cis-[Pd(L^1-*S*,*O*)$_2$]	—	—	—	—	−8.4	11.2
cis-[Pt(L^2-*S*,*O*)$_2$]	—	47	20	28	−12.4	8.5
cis-[Pd(L^2-*S*,*O*)$_2$]	—	—	—	—	−8.3	10.8
cis-[Pt(L^3-*S*,*O*)$_2$]	−2764	45	21	31	−11.9	9.5
cis-[Pd(L^3-*S*,*O*)$_2$]	—	—	—	—	−7.9	11.9
			$^3J[^{103}Rh–^{13}C(2'')]$/Hz [c]			
fac-[Rh(L^2-*S*,*O*)$_3$]	—	—	1.9	—	−5.8	12.1
fac-[Rh(L^3-*S*,*O*)$_3$]	—	—	<1	—	−8.3	12.7

[a] Measured at 30 °C relative to external reference of 500 mg cm^{-3} H_2PtCl_6 in 30% (v/v) D_2O/1 M HCl, set to $\delta(^{195}Pt)$ = 0 ppm. [b] Defined as $\Delta = (\delta^{13}C_{complex} - \delta^{13}C_{ligand})$, see text, upfield (−) and downfield (+) shift. [c] Line-widths of octahedral Rh(III) complexes are narrow, typically <0.7 Hz, in contrast to square-planar Pt(II) complexes.

shift trends for some carbon atoms on complex formation. Notable are the relatively large displacements, Δ [defined as: $\Delta = (\delta^{13}C_{complex} - \delta^{13}C_{ligand})$], observed for the ^{13}C shifts of the thiocarbonyl and carbonyl atoms, on going from unbound ligand to the metal complex. Thus the C(S) and the C(O) carbon resonances undergo relatively large average *upfield* and *downfield* displacements of 12.4 ± 0.6 and 8.98 ± 0.49 ppm, respectively, for the Pt(II) complexes. The corresponding shift displacements for the Pd(II) complexes are 8.2 ± 0.3 and 11.3 ± 0.5 ppm, respectively, while for the Rh(III) complexes these are 5.7 ± 0.1 and 12.4 ± 0.4 ppm. The unambiguous assignment of these resonances to the C(S) and C(O) atoms in the ligands and the platinum complexes is based on nuclear Overhauser enhanced $^1H–^{13}C$ coupled spectra. Thus, for example, in the *cis*-[Pt(L^3-*S*,*O*)$_2$] complex, proton coupled resonance of C(O) [$\delta(^{13}C)$ = 166.6 ppm)] appears as a 10-line multiplet arising from $^3J(^1H–^{13}C)$ = 4.2 Hz coupling due to nine equivalent H atoms of the 2,2-dimethylpropyl moiety. The corresponding C(S) resonance [$\delta(^{13}C)$ = 183.5 ppm] is a 5-line multiplet arising from $^3J(^1H–^{13}C)$ = 3.5 Hz coupling due to two sets of protons arising from two inequivalent CH_2 groups of the piperidyl moieties.

The relatively large shift displacements, Δ, for C(O) and C(S) in these complexes are consistent with extensive delocalisation of a single electron within the six-membered M–S–C–N–C–O chelate ring of these complexes. Interestingly, the general trend in Δ follows the order Pt(II) > Pd(II) > Rh(III) for C(S), the reverse order being observed for C(O). Given that C(O) and C(S) are bonded directly to the metal centre through an oxygen and sulfur donor atom, respectively, it is tempting to speculate whether these shift displacement vlaues reflect the relative order of HASAB 'softness'[20] of the metal centre in the order Pt(II) > Pd(II) > Rh(III).

In the case of the *cis*-[Pt(L^n-*S*,*O*)$_2$] complexes, the existence of, and trends observed in, the well resolved $^nJ(^{195}Pt–^{13}C)$ 'satellite' resonances assist in the unambiguous assignment of some of the ^{13}C resonances in these complexes. Inspection of the data in Table 2 shows that relatively broad $^2J(^{195}Pt–^{13}C)$ coupling satellites are only observed for the thio-carbonyl atom (average 46 ± 1 Hz) whereas that for the carbonyl atom is not resolved (being <8 Hz, the line-width at the base of this ^{13}C resonance); additional $^3J(^{195}Pt–^{13}C)$ couplings of 20.8 ± 0.4 Hz at C(2″), and $^4J(^{195}Pt–^{13}C)$ couplings of 30.7 ± 0.8 Hz are visible for only *one* of the magnetically non-equivalent *N*-alkyl CH_2 (for L^2/L^3) or the CH_3 (for L^1) moieties in the ^{13}C NMR spectra of the co-ordinated ligand. This four-bond coupling allows for the unambiguous assignment of this resonance to the C-atoms of the *N*-alkyl CH_2 (for L^2/L^3) or the CH_3 (for L^1) groups, which adopt a planar 'W' configuration with respect to the platinum atom, due to restricted rotation about this bond on the NMR time scale, as a result of the partial double-bond character of the C–N bond of the C(S)–N(CH$_2$–)$_2$ moiety.[19,21]

Crystal structure of *cis*-bis[*N*-piperidyl-*N′*- (2,2-dimethylpropyl)-thioureato]platinum(II)

Fig 1 shows the molecular structure of *cis*-[Pt(L^3-*S*,*O*)$_2$], confirming the expected *cis* configuration. Table 1 gives the relevant crystal structure and refinement details for this complex, whereas selected bond lengths and angles are given in Fig. 1. Closer inspection of the crystal structure of *cis*-[Pt(L^3-*S*,*O*)$_2$] shows that the Pt–S–C–N–C–O chelate rings are essentially planar (maximum deviation from perfect planarity is 0.15 Å) but that the two chelate rings differ slightly from each other as reflected in the small differences in the Pt–S1A and Pt–S1 as well as the Pt–O1A and Pt–O1 bond lengths [2.2301(14) compared with 2.2422(11) Å, and 2.010(3) compared with 2.033(3) Å, respectively]; these small differences are also reflected in the other pertinent bond lengths and bond angles. The origin of these small differences may be due to packing effects, which result in the two piperidyl moieties having substantially different orientations with respect to the planar chelate rings of the complex. These differing orientations are illustrated by the significant differences in the torsion angles C(2A)–N(1A)–C(1A)–N(2A) [−177.7(4)°] compared with C(2)–N(1)–C(1)–N(2) [167.7(4)°], and C(3A)–N(2A)–C(1A)–N(1A) [0.2(6)°] and C(3)–N(2)–C(1)–N(1) [1.8(6)°]. The conformations of the two piperidyl rings also differ as shown by the torsion angles N(2A)–C(3A)–C(4A)–C(5A) [−55.3(6)°] and N(2)–C(3)–C(4)–C(5) [−58.7(6)°] and C(3A)–C(4A)–C(5A)–C(6A) [53.1(7)°] and C(3)–C(4)–C(5)–C(6) [−57.9(5)°].

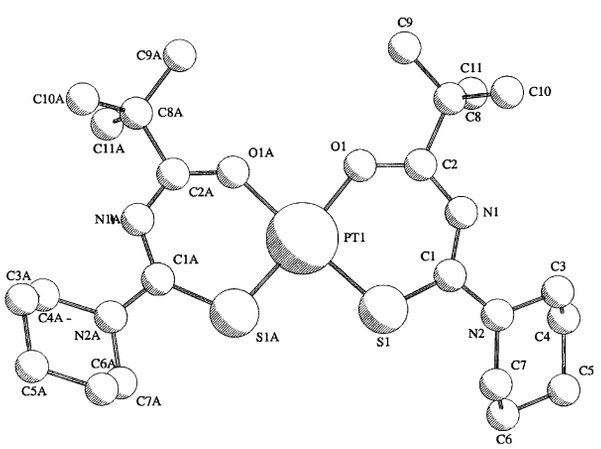

Fig. 1 Molecular structure of *cis*-bis[*N*-piperidyl-*N′*-(2,2-dimethylpropyl)thioureato]platinum(II). Some important bond lengths (Å) and angles (°) are: Pt(1)–O(1A) 2.010(3), Pt(1)–O(1) 2.033(3), Pt(1)–S(1A) 2.2301(14), Pt(1)–S(1) 2.2422(11), C(2)–N(1) 1.308(6), C(2A)–N(1A) 1.318(5), C(2)–O(1) 1.258(5), C(2A)–O(1A) 1.258(5), C(1)–N(1) 1.346(5), C(1A)–N(1A) 1.350(5), C(1)–S(1) 1.744(4), C(1A)–S(1A) 1.726(4), C(1)–N(2) 1.332(6), C(1A)–N(2A) 1.350(5); O1A–Pt1–O1 81.95(12), O1A–Pt1–S1A 94.53(8), O1–Pt1–S1A 175.89(10), O1A–Pt1–S1 176.63(9), O1–Pt1–S1 94.93(9), S1A–Pt1–S1 88.63(4), C1A–S1A–Pt1 107.95(13), C2–O1–Pt1 128.2(3), C1–S1–Pt1 106.33(15), C2A–O1A–Pt1 130.3(3), C2A–N1A–C1A 126.8(3).

Nevertheless, the average Pt–S, and Pt–O bond lengths, as well as the O–Pt–S, O–Pt–O and S–Pt–S angles of *cis*-[Pt(L^3-*S*,*O*)$_2$] do not differ significantly from the corresponding values observed in the related *cis*-bis[*N*,*N*-dibutyl-*N*-(benzoyl)thioureato]platinum(II)[7b] complex, suggesting that substitution of the aromatic group by the pivaloyl [(CH$_3$)$_3$–] moiety in *cis*-[Pt(L^3-*S*,*O*)$_2$] does not significantly affect the (delocalized) electron distribution in the Pt–S–C–N–C–O chelate ring.

Crystal structure of *fac*-tris[*N*-pyrrolidyl-*N′*-(2,2-dimethylpropyl)thioureato]rhodium(III)

The molecular structure of the *fac*-[Rh(L^2-*S*,*O*)$_3$]·CHCl$_3$ in Fig. 2(a) shows the Rh atom of the complex to lie at the centre

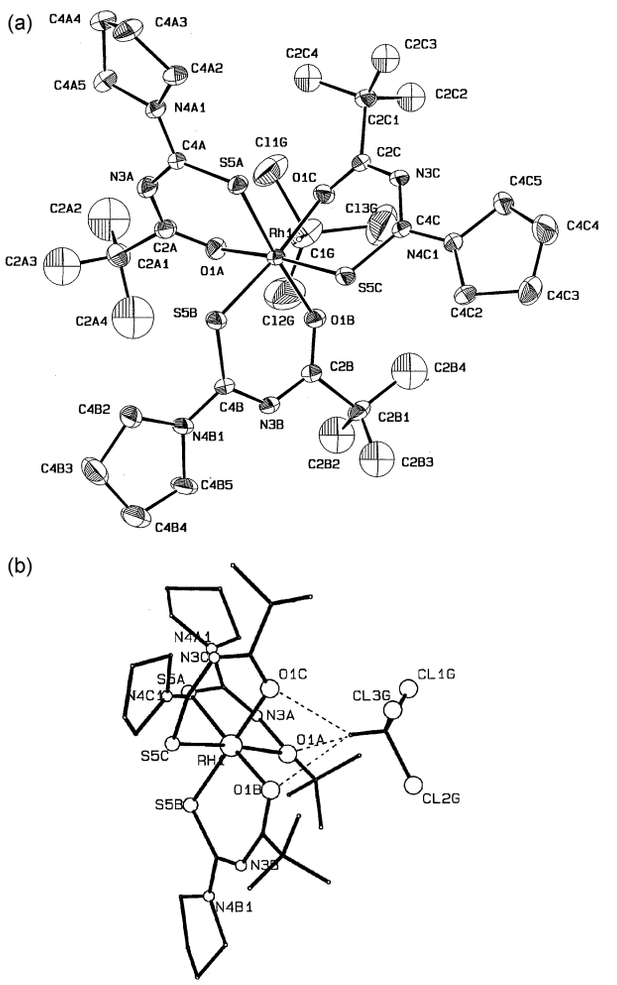

Fig. 2 (a) Molecular structure of *fac*-tris[*N*-pyrrolidyl-*N′*-(2,2-dimethylpropyl)thioureato]rhodium(III), with some important bond lengths (Å) and angles (°): Rh1–O1A 2.051(4), Rh1–O1B 2.058(4), Rh1–O1C 2.070(4), Rh1–S5B 2.2654(17), Rh1–S5C 2.2686(17), Rh1–S5A 2.2749(17), C4A–S5A 1.742(6), O1A–C2A 1.262(7), C4B–S5B 1.723(6), O1B–C2B 1.258(7), O1C–C2C 1.257(7), C4C–S5C 1.731(6); O1A–Rh1–O1C 86.79(16), O1B–Rh1–O1C 87.72(16), O1A–Rh1–S5B 89.43(13), O1B–Rh1–S5B 95.85(12), O1C–Rh1–S5B 174.61(11), O1A–Rh1–S5C 173.63(12), O1B–Rh1–S5C 87.96(13), O1C–Rh1–S5C 94.79(11), S5B–Rh1–S5C 89.39(6), O1A–Rh1–S5A 95.25(13), O1B–Rh1–S5A 176.29(11), O1C–Rh1–S5A 88.84(13), S5B–Rh1–S5A 87.69(6), S5C–Rh1–S5A 90.96(6), C2A–O1A–Rh1 124.5(4). (b) Schematic representation of the trifurcated $Cl_3C–H\cdots O$ (mean distance 3.47 ± 0.11 Å) contacts between the $CHCl_3$ molecule and one face of the *fac*-[Rh(L^2-*S*,*O*)$_3$] complex.

of an octahedron defined by three S and three O donor atoms in a facial arrangement of the bound ligand. The relevant crystal structure and refinement details of the complex are given in Table 1. Interestingly, the *fac*-[Rh(L^2-*S*,*O*)$_3$] complex in the crystal lattice is in close contact with a molecule of chloroform, in which the H-atom of the latter is directed toward the face of the octahedron defined by three co-ordinated oxygen atoms, presumably through a weak trifurcated hydrogen bond [ClG–H1G ··· O1A 3.45(1) Å, 143°; ClG–H1G ··· O1B 3.60(1) Å, 142°; ClG–H1G ··· O1C 3.37 Å, 140°], shown in Fig. 2(b). The average Rh^{III}–O and Rh^{III}–S bond lengths, at 2.060 ± 0.009 and 2.269 ± 0.005 Å, respectively, are quite similar to the Rh^{III}–O and Rh^{III}–S bond lengths for *tris*-[*N*,*N*-diethyl-*N*′-(benzoyl)-thioureato]rhodium(III) at 2.033(5) and 2.284(3) Å, respectively.[22] It is notable that the Rh^{III}–S bond length of *ca.* 2.270 Å is virtually identical to the average and Pt^{II}–S distance (2.271 Å) found for *cis*-[Pt(L^3-*S*,*O*)$_2$] (Fig. 1), whereas the Rh^{III}–O bond length is somewhat longer than the average Pt^{II}–O distance. On the other hand, the two partial double N–C bond lengths in the chelate ring of the ligand for *fac*-[Rh(L^2-*S*,*O*)$_3$] differ significantly from the corresponding lengths for the *cis*-[Pt(L^3-*S*,*O*)$_2$] complex {mean bond lengths N3–C(O) 1.329 ± 0.004 Å and N3–C(S) 1.326 ± 0.015 Å in *fac*-[Rh(L^2-*S*,*O*)$_3$] compared with the corresponding distances 1.314 ± 0.007 and 1.348 ± 0.011 Å in *cis*-[Pt(L^3-*S*,*O*)$_2$]}.

Separation of *cis*-[M(L^n-*S*,*O*)$_2$] and *fac*-[Rh(L^2-*S*,*O*)$_3$] by means of RP-HPLC

The facile formation of stable, essentially pure *cis*-[M(L^n-*S*,*O*)$_2$] [for *n* = 1–3; M = Pt(II), Pd(II)] and *fac*-[Rh(L^n-*S*,*O*)$_3$] (*n* = 2, 3) with ligands described in this work, as well as their reasonable water solubility and high molar absorptivities, are ideal properties for their potential RP-HPLC separations. This is confirmed by a systematic investigation of the separation properties of *cis*-[M(L^2-*S*,*O*)$_2$] [for M = Pt(II), Pd(II)] and *fac*-[Rh(L^2-*S*,*O*)$_3$] complexes, which readily resulted in chromatograms as shown in Fig. 3, using a 150 × 4.6 mm, 5 μm C_{18}-ODS column, with 90:10 (%v/v) acetonitrile:0.1 M sodium acetate (pH 6) buffer as mobile phase, at ambient temperatures. Optimum separation conditions were obtained by systematically varying the mobile-phase composition, buffer pH and the careful selection of column type used (a 'standard' C_{18}-HPLC ODS column without treatment for residual silanol-group capping resulted in some severe peak-tailing effects and lower overall chromatographic resolution). Under these conditions, the unbound ligands are not strongly retained, and elute from the column within 1–3 min after injection.

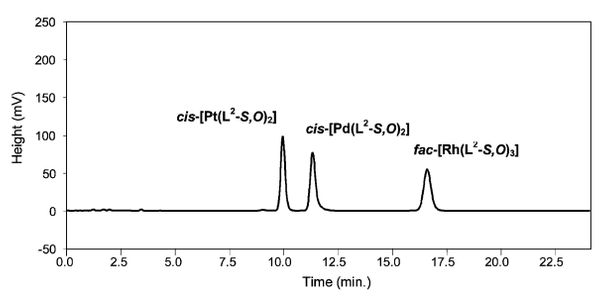

Fig. 3 Representative RP-HPLC chromatogram of a 20 μl aliquot of an acetonitrile solution containing 29, 20 and 20 μg cm^{-3} of pure *cis*-[Pt(L^2-*S*,*O*)$_2$], *cis*-[Pd(L^2-*S*,*O*)$_2$] and *fac*-[Rh(L^2-*S*,*O*)$_3$], respectively. Mobile phase, 90:10 (%v/v) acetonitrile:0.1 M sodium acetate buffer (pH 6), flow rate 1.0 cm^3 min^{-1}; column 150 × 4.6 mm, 5 μm LUNA C_{18}-ODS; photometric detection at λ = 254 nm, at ambient temperature.

Excellent linear calibration curves of peak area *vs.* complex concentration in the concentration range 0–40 μg cm^{-3} could readily be obtained for pure Pt(II), Pd(II) and Rh(III) complexes of HL^2 (freshly dissolved in acetonitrile) using these chromatographic conditions with photometric UV detection at 254 nm. The determined limits of detection (LOD) and quantification (LOQ) shown in Table 3 indicate that, in principle, in the UV absorption region (254–264 nm) this technique allows for the quantitative determination of Pt(II), Pd(II) and Rh(III) at trace levels. Quantification is nevertheless possible over a much wider range of wavelengths (typically in the range 254–390 nm), albeit at lower overall sensitivity as the monitoring wavelength for chromatographic peaks is shifted to higher λ. Shown in Table 3 are the recoveries achieved for synthetic test solutions as well as the method validation data for determining Pt(II) and Pd(II) concentrations, discussed further below.

Sample preparation and method validation

A key objective of this study was to develop a practically useful RP-HPLC method of determination of Pt(II) and Pd(II) in acidic process streams. To this end, it was necessary to develop simple, yet robust, sample preparation methodology. Ideally such methodology should fulfil a number of stringent criteria *viz.*: (i) it should be simple and robust, for practical application; (ii) the complex formation process should be rapid, quantitative and preferably yield mono-isomeric metal complexes; (iii) it should be compatible with acidic aqueous process streams; (iv) it should yield complexes which separate rapidly and with good resolution; (v) it should allow for accurate quantification of metal ions over a high dynamic range; and (vi) be free from interferences. The preliminary separability of pure *cis*-[Pt(L^n-*S*,*O*)$_2$], *cis*-[Pd(L^n-*S*,*O*)$_2$] and *fac*-[Rh(L^n-*S*,*O*)$_3$] complexes shown in Fig. 3 suggested that relatively hydrophilic ligands HL^n examined in this work could be useful for an '*in situ*' complex formation method in homogeneous water–acetonitrile mixtures, followed by salt-induced phase separation and RP-HPLC. This was indeed found to be the case using a simple sample preparation method shown schematically in Fig. 4. Essentially, the complex formation between HL^n and the chloro-anionic complexes of Pt(II), Pd(II) and Rh(III) in dilute HCl takes place in a homogeneous acid–acetonitrile phase, followed by salt-induced phase separation and pH adjustment, to yield an acetonitrile-rich phase in which the *cis*-[M(L^n-*S*,*O*)$_2$] and *fac*-[Rh(L^n-*S*,*O*)$_3$] complexes are pre-concentrated, ready for RP-HPLC analysis.

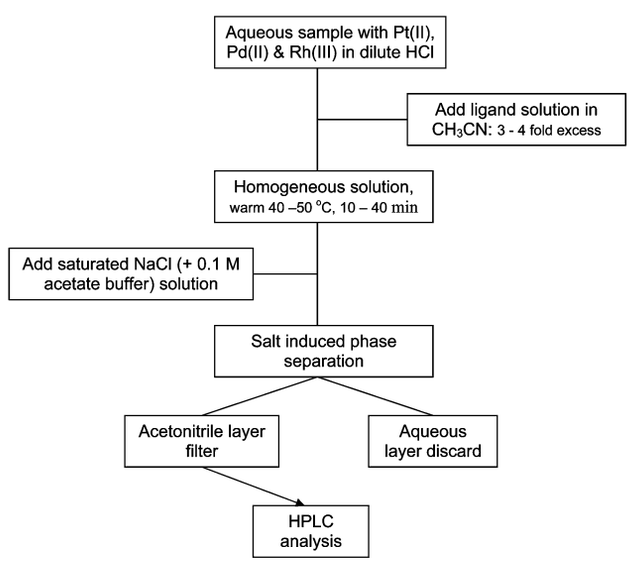

Fig. 4 Schematic representation of the sample preparation methodology suitable for acidic (0–0.2 M HCl) aqueous solutions containing $PtCl_4^{2-}$, $PdCl_4^{2-}$ and $RhCl_3 \cdot 3H_2O$, which consists of complex formation, pre-concentration followed by salt induced phase-separation, prior to injection of the acetonitrile-rich phase into the HPLC system.

Table 3 Representative limits of detection (LOD) and quantification (LOQ) for the quantitative RP-HPLC determination of *cis*-[M(L^2-*S*,*O*)$_2$] [for M = Pt(II), Pd(II)] and *fac*-[Rh(L^2-*S*,*O*)$_3$], under near optimum conditions. Shown also are recovery and validation experiments for acidic solutions containing known amounts of Pt(II/IV) and Pd(II). The HPLC methodology is not suitable for Pt(IV), but reduction of the latter allows for satisfactory results

		Detection/quantification limits[a]			Recovery[b]		Validation[c]	
Sample		λ_{max}/nm	LOD/μg cm^{-3}	LOQ/μg cm^{-3}	Taken/μg cm^{-3}	Found/μg cm^{-3}	HPLC/μg cm^{-3}	ICPAES[d]/μg cm^{-3}
cis-[Pt(L^2-*S*,*O*)$_2$]		258	0.03	0.15	103.4	102 ± 1.8	—	—
cis-[Pd(L^2-*S*,*O*)$_2$]		276	0.02	0.08	61.9	64 ± 1.1	—	—
'Unknown 1'	Pt	—	—	—	—	—	4.8[e]	44 ± 0.8
	Pd	—	—	—	—	—	25 ± 1.4	24 ± 0.6
'Unknown 2'	Pt	—	—	—	—	—	40 ± 1.0	44 ± 0.3
	Pd	—	—	—	—	—	25 ± 1.4	24 ± 0.2
fac-[Rh(L^2-*S*,*O*)$_3$]		264	0.03	0.12	—	—	—	—

[a] LOD and LOQ calculated as defined in ref. 23. [b] Determined in triplicate by sample preparation methodology, followed by HPLC using calibration graphs separately prepared from known aqueous standards. [c] 'Blind' samples prepared from aqueous standards; Pt and Pd concentration compared by two methods. [d] Inductively-Coupled Plasma Atomic Emission Spectroscopy. [e] Pt present as Pt(IV) in 'unknown 1'; reduction with excess tin(II) chloride, prior to HPLC in 'unknown 2'.

Table 4 Influence of ligand structure on the RP-HPLC chromatographic separation characteristics of *cis*-[M(L^n-*S*,*O*)$_2$] [for M = Pt(II), Pd(II), *n* = 1–3] and related complexes [mobile phase, 90:10 (%v/v) acetonitrile:0.1 M sodium acetate buffer (pH 6), flow rate 1.0 cm^3 min^{-1}; column 150 × 4.6 mm, 5 μm LUNA C_{18}-ODS; photometric detection at λ = 254 nm, ambient temperature]. Where the resolution, R_s, for Pt(II) and Pd(II) complexes is given, these samples where prepared by the methodology described in Fig. 4; in other cases retention times for pure complexes in acetonitrile solutions are given

Ligand		Retention times[a]			Resolution[b]
R	R′, R′	t_{HL}/min	t_{Pt}/min	t_{Pd}/min	R_s(Pt/Pd)
$(CH_3)_3C$– (pivaloyl)	Pyrrolidyl	—	18.0	20.9	2.7
$(CH_3)_3C$–	Ethyl	1.8	17.1	20.2	3.4
$(CH_3)_3C$–	*N*-Morpholine	1.7	6.7	7.6	1.9
C_6H_5– (benzoyl)	Ethyl	1.7	11.0	12.1	1.8
C_6H_5–	n-Butyl	2.4	11.1	12.1	1.2
C_6H_5–	*N*-Morpholine	1.7	4.9	—	—
C_6H_5–	*N*-Piperidine	2.6	16.2[c]	—	—
3,4,5-Trimethoxybenzoyl-	Ethyl	1.9	8.0[c]	8.4[c]	0.8
4-Cl–C_6H_4–	*N*-Piperidine	2.3	13.7[c]	—	—
4-NO_2–C_6H_4–	*N*-Piperidine	2.6	15.9[c]	—	—
$C_{10}H_7$– (naphthoyl)	Ethyl	1.8	19.5	22.1	1.9

[a] Zorbax Eclipse XDB-C18 column, 4.6 × 150 mm, 5 μm; 90% acetonitrile, 10% 0.1 M acetate buffer, 1 cm^3 min^{-1}, at room temperature. [b] Determined[23] from $R_s = 2(t_{Pd} - t_{Pt})/W_{Pt} + W_{Pd}$. [c] Chromatographic peaks are significantly broader than others under these conditions; two additional minor peaks are evident.

A thorough investigation of the various factors which might influence the sample preparation methodology, such as the time for complex formation, the reaction temperature, the tolerable initial HCl concentration, the eluent composition, buffer concentration and pH, was undertaken, leading to the optimum sample preparation conditions shown in Fig. 4. In general, for $PtCl_4^{2-}$ and $PdCl_4^{2-}$ the tolerable initial acid concentrations in the sample solution can range from 0 to 0.2 M HCl; concentrations > 0.2 M HCl lead to progressively broader chromatographic peaks, as well as to slight increases in peak area for Pd(II) complexes, and decreases in peak area for Pt(II) complexes, probably reflecting substitution kinetic differences between Pd(II) and Pt(II) chloro-anions at higher HCl concentrations. At room temperature, the rate of complex formation is, however, relatively rapid in the presence of a 3–10-fold excess of ligand, and a reaction time of between 10 and 20 min is found to be adequate for the quantitative recovery of initial Pt(II) and Pd(II) concentrations of less than 100 μg cm^{-3}. Warming the reaction mixture to 45–50 °C leads to a reduction of complex formation time to less than 10 min. Unfortunately, to achieve semi-quantitative results for Rh(III), the overall rate of complex formation was found to be too slow at room temperature; this requires the warming of the sample–acetonitrile mixture to between 60 and 80 °C for more than 40 min. For this reason, we will limit further discussion of this method to Pt(II) and Pd(II) in the present paper.

As part of this study, we undertook an investigation of the effect of ligand structure on the RP-HPLC separation characteristics of *cis*-[Pt(L^n-*S*,*O*)$_2$] and *cis*-[Pd(L^n-*S*,*O*)$_2$] complexes, in an attempt to identify the most suitable ligand, as well as the structural elements most favourable for the metal complex separation. The retention behaviour of freshly prepared acetonitrile solutions of the new series of pure *cis*-[Pt(L^n-*S*,*O*)$_2$] complexes first described in this paper, as well as similar complexes previously prepared,[19b] was thus examined in some detail. The overall chromatographic results from these experiments are shown in Table 4, listing the retention times of ligand and their corresponding complexes. Shown also is R_s, the relative chromatographic resolution[23] of the separation of the corresponding *cis*-[Pt(L^n-*S*,*O*)$_2$] and *cis*-[Pd(L^n-*S*,*O*)$_2$] complexes, as prepared '*in situ*' with the methodology described in Fig. 4. The retention times for all the ligands studied were less than 3 min, suggesting that the presence of excess ligand will not interfere with the separation of the metal complexes. Moreover, it is clear that the 'best' chromatographic resolution is achieved for the *cis*-[Pt(L^2-*S*,*O*)$_2$] and *cis*-[Pd(L^2-*S*,*O*)$_2$] complexes derived from the *N*-pyrrolidyl-*N*′-(2,2-dimethylpropanoyl)thiourea, although very similar separation characteristics are obtained for complexes derived from *N*,*N*-diethyl-*N*′-(2,2-dimethylpropanoyl)thiourea. Inspection of the retention times obtained for variously substituted *N*,*N*-dialkyl-*N*′-(acyl)aroylthioureas shows an interesting but complicated

relationship between ligand structure and complex retention behaviour. It is indeed interesting that the ostensibly isostructural *cis*-[Pt(L^n-*S*,*O*)$_2$] and *cis*-[Pd(L^n-*S*,*O*)$_2$] complexes separate so well, the palladium complex being generally more retained by the stationary phase than the platinum analogue. Moreover, complexes of substituted benzoyl derivatives appear to result in unfavourable separations, while simple *N*,*N*-diethyl-*N*′-benzoylthiourea complexes give good separations, despite the relatively poor absolute solubility of this ligand in water–acetonitrile mixtures. Data in Table 4 suggest that the *N*,*N*-dialkyl- substituents appear to have a relatively more significant effect on the separation of their complexes, as shown for the series of *N*-pyrrolidyl, *N*,*N*-diethyl- and *N*-morpholine derivatives of *N*′-(2,2-dimethylpropanoyl)thiourea. The relatively short retention time of Pt complexes of *N*-morpholine-*N*′-(2,2-dimethylpropanoyl)thiourea (t_{Pt} = 6.7 min) and *N*-morpholine-*N*′-benzoylthiourea (t_{Pt} = 4.9 min) are noteworthy, suggesting that the expected hydrophilicity of the morpholine substituent plays a role. In any event, it is clear that ligand structure has a significant effect on the RP-HPLC separation properties of Pt and Pd complexes, but a fuller understanding of these effects must await further study.

An interesting and significant observation concerning the *cis–trans* isomer distribution of [Pt(L^2-*S*,*O*)$_2$] complexes has been made from the chromatographic behaviour of solutions of *cis*-[Pt(L^2-*S*,*O*)$_2$] prepared in acetonitrile. A necessary condition for a practically useful HPLC method of Pt(II) and Pd(II) determination is the formation of stable, mono-isomeric complexes. In general we have found an overwhelming tendency of *N*,*N*-dialkyl-*N*′-(acyl)aroylthioureas to yield *cis*-[Pt(L^2-*S*,*O*)$_2$] complexes;[19b] the only well-authenticated *trans*-Pt(II) complex described in the literature is *trans*-bis[*N*,*N*-(di-n-butyl)-*N*′-naphthoylthioureato]platinum(II), which forms only as a minor product (*ca.* 15%).[7c] Nevertheless, we find that while repeated injection of freshly made acetonitrile solutions of, for example, pure *cis*-[Pt(L^1-*S*,*O*)$_2$], gives only a single chromatographic peak, prolonged standing of these solutions at room temperature followed by injection into the HPLC system results in the appearance of a small additional peak in the chromatogram, as illustrated in Fig. 5. This small peak has a shorter retention time than the major peak due to the authentic *cis*-[Pt(L^1-*S*,*O*)$_2$] complex. These chromatograms suggest that, on standing, the initially pure *cis*-complex slowly isomerises to the *trans* analogue. Convincing evidence that the second peak is due to the *trans*-[Pt(L^1-*S*,*O*)$_2$] isomer is obtained from the electrospray mass spectrum (ES-MS) of these peaks after direct injection into the ES-MS spectrometer after elution from the HPLC column. The resulting mass spectra show very similar fragmentation patterns, together with two strong clusters of peaks at *m*/*z* values of 568, 569, 570, 571, 572 for *both* chromatographic peaks. These *m*/*z* values correspond well to the calculated average *m*/*z* value of 570.67 for the MH$^+$ ion. Moreover, the UV spectra of these two chromatographic peaks (obtained using a diode array detector) are similar, strongly suggestive of isomerisation.

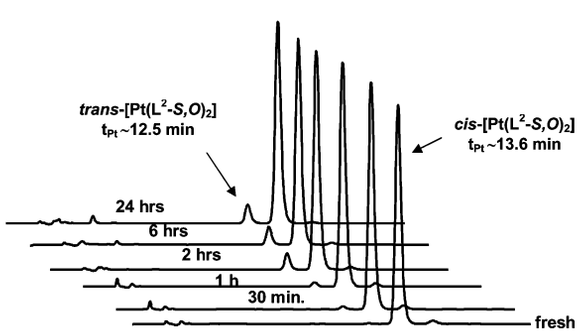

Fig. 5 Chromatogram showing the apparent isomerisation of a freshly prepared solution of *cis*-[Pt(L^1-*S*,*O*)$_2$] in pure acetonitrile, after standing at ambient temperature for the indicated times [mobile phase 90:10 (%v/v) acetonitrile:0.1 M sodium acetate buffer (pH 6), flow rate 1.0 cm^3 min^{-1}; column 150 × 4.6 mm, 5 μm LUNA C_{18}-ODS; photometric detection at λ = 254 nm, ambient temperature]. The peak at $t_{Pt} \approx$ 12.4 min is ascribed to *trans*-[Pt(L^2-*S*,*O*)$_2$], on the basis of ES-MS and its absorption spectrum (see text).

This phenomenon is most pronounced for the *cis*-[Pt(L^1-*S*,*O*)$_2$], showing the most rapid apparent isomerisation at room temperature, these solutions reaching a steady state within *ca.* 24–36 h. For the related *cis*-[Pt(L^2-*S*,*O*)$_2$] and *cis*-*bis*[*N*,*N*-diethyl-*N*′-(2,2-dimethylpropanoyl)thioureato]-platinum(II) the second chromatographic peak develops more slowly, these solutions requiring more than one week of standing before reaching a steady state. All other complexes studied in this work appear to isomerise much more slowly, although a systematic time dependence study has not yet been carried out. This observation is very interesting in view of the paucity of structurally characterised examples of *trans*-[Pt(L^n-*S*,*O*)$_2$] complexes in the literature. Fortunately, however, in pure acetonitrile the apparent rate of isomerisation of *cis*-[Pt(L^n-*S*,*O*)$_2$] is relatively slow, so that freshly prepared solutions of *cis*-[Pt(L^n-*S*,*O*)$_2$] only show a significant amount of the *trans* isomer (>1%) after standing for longer than *ca.* 1–2 h for the complexes mentioned above for which isomerisation is evident at all. No such phenomenon has been observed for the corresponding Pd(II) complexes. Significantly, however, we find that if the Pt(II) and Pd(II) complexes are prepared freshly according to the '*in situ*' procedure described in Fig. 4, no evidence of such apparent isomerisation is observed in the chromatograms of the acetonitrile-rich phase produced after salt-induced phase separation. This finding suggests that in the presence of significant quantities of water during the complex formation process, only *cis*-[Pt(L^n-*S*,*O*)$_2$] isomers are formed, possibly due to the relatively high dielectric constants of water–acetonitrile mixtures compared with pure acetonitrile solutions. It is not unreasonable to suppose that the *cis* complexes with a higher dipole moment are favoured in high dielectric constant (water-containing) solvent mixtures. This phenomenon, which is of considerable fundamental interest to us, is currently being studied more thoroughly, and will be reported on further elsewhere.

In order to test the applicability of the methodology described above for the simultaneous quantitative determination of Pt(II) and Pd(II) in dilute HCl, solutions containing known amounts of Pt(II) and Pd(II) in the range 1–400 μg cm^{-3} in 0.1M HCl were treated according to a standardised sample preparation procedure (Fig. 4) for the ligand *N*-pyrrolidyl-*N*′-(2,2-dimethylpropanoyl)thiourea (HL^2), and subjected to RP-HPLC analysis, yielding typical chromatograms for mixtures of (a) 50 μg cm^{-3} Pd + 4 μg cm^{-3} Pt and (b) 50 μg cm^{-3} Pt and 0.5 μg cm^{-3} Pd, as shown in Fig. 6. Excellent linear calibration graphs were obtained for these solutions in the concentration range of 0–330 μg cm^{-3} and 0–400 μg cm^{-3} for Pd(II) and Pt(II), respectively. Moreover, the results of recovery and method validation experiments (Table 3) show convincingly that Pt(II) and Pd(II) in dilute HCl can accurately be determined with this method to within *ca.* 3% at a relative standard deviation of *ca.* 2% for initial Pt(II) and Pd(II) concentrations >25 μg cm^{-3}. As expected, the precision of determination decreases to between 6 and 10% as the initial metal ion concentration decreases to below 6 μg cm^{-3} in the aqueous phase. Nevertheless, with photometric detection at 254 nm, 0.5 μg cm^{-3} Pd(II) in the presence of 50 μg cm^{-3} Pt(II), and 2 μg cm^{-3} Pt(II) in the presence of 50 μg cm^{-3} Pd(II) can readily be determined to within an acceptable relative standard deviation at this level of concentration.

It is clear from preliminary results in Table 3 that the method developed for Pt(II) is, at present, not suitable for Pt(IV) chlorides. Nevertheless, if a reduction step of Pt(IV) to Pt(II) is carried out [with tin(II) chloride solution] prior to addition of the ligand, then reasonably satisfactory quantitative determination of Pt by means of RP-HPLC is possible.

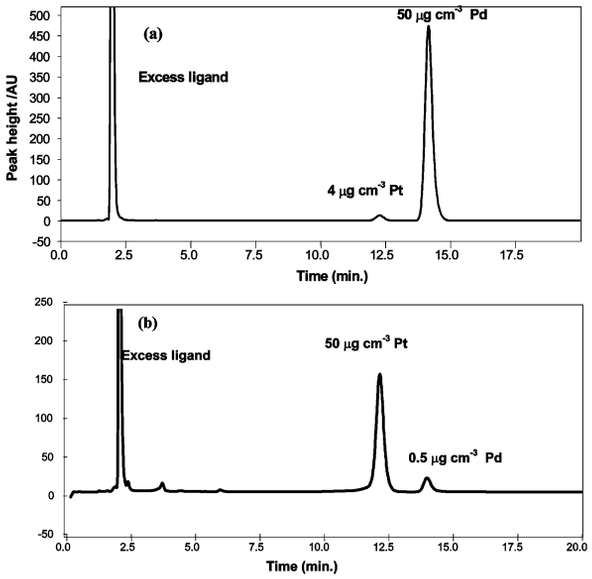

Fig. 6 Chromatograms for the determination of Pt(II) and Pd(II) in dilute HCl solutions after sample preparation using the methodology developed in this paper, using *N*-pyrrolidyl-*N′*-(2,2-dimethylpropyl)-thiourea as ligand, and optimised RP-HPLC conditions: (a) 4 μg cm^{-3} Pt + 50 μg cm^{-3} Pd; (b) 50 μg cm^{-3} Pt + 0.5 μg cm^{-3} Pd. (Column 150 × 4.6 mm, 5 μm LUNA C_{18}-ODS; mobile phase 90:10 (%v/v) acetonitrile:0.1 M acetate buffer (pH 6); flow rate 1.0 cm^3 min^{-1}; detection $\lambda = 254$ nm.)

Conclusions

The favourable physicochemical properties of relatively hydrophilic *N*,*N*-dialkyl-*N′*-(2,2-dimethylpropyl)thioureas (HL^n) ($n = 1$, *N*,*N*-dimethyl-; $n = 2$, *N*-pyrrolidyl-; $n = 3$, *N*-piperidyl-) and their ready formation of stable, mono-isomeric *cis*-[Pt(L^n-*S*,*O*)$_2$] and *cis*-[Pd(L^n-*S*,*O*)$_2$] complexes makes these compounds suitable for the quantitative determination of traces of these metal ions in hydrochloric acid. Simple and robust sample preparation methodology has been developed, in which is involved an *in situ* complex formation in a homogeneous acetonitrile–hydrochloric acid phase, followed by subsequent salt (NaCl) induced phase separation and analysis. A study of the effect of ligand structure on the separation behaviour of *cis*-[M(L^n-*S*,*O*)$_2$] of Pd(II) and Pt(II) complexes has been undertaken, showing that the nature of the ligand has a significant influence on the separation characteristics of these complexes.

Acknowledgements

Financial support from the National Research Foundation (GUN 2046827), THRIP (Project no. 1562), Angloplatinum Ltd., AECI Ltd (Fellowship to A. N. M.) and the University of Stellenbosch is gratefully acknowledged.

References

1 L. Beyer, E. Hoyer, J. Liebscher and H. Hartmann, *Z. Chem.*, 1981, **21**, 81.
2 K.-H. König, M. Schuster, B. Steinbrech, G. Schneeweis and R. Schlodder, *Fresenius Z. Anal. Chem.*, 1985, **321**, 457; M. Schuster, *Fresenius Z. Anal. Chem.*, 1986, **324**, 127; P. Vest, M. Schuster and K.-H. König, *Fresenius Z. Anal. Chem.*, 1989, **335**, 759.
3 K.-H. König, M. Schuster, G. Schneeweiss and B. Steinbrech, *Fresenius Z. Anal. Chem.*, 1985, **325**, 621.
4 M. Schuster, *Fresenius Z. Anal. Chem.*, 1992, **342**, 791.
5 M. Schuster and E. Unterreitmaier, *Fresenius' J. Anal. Chem.*, 1993, **346**, 630; M. Schuster and E. Unterreitmaier, *Anal. Chim. Acta*, 1995, **309**, 339.
6 M. Schwarzer and M. Schuster, *Anal. Chim. Acta*, 1996, **328**, 1.
7 (*a*) K. R. Koch, C. Sacht, T. Grimmbacher and S. Bourne, *S. Afr. J. Chem.*, 1995, **48**, 71; (*b*) K. R. Koch, A. Irving and M. Matoetoe, *Inorg. Chim. Acta*, 1993, **206**, 193; (*c*) K. R. Koch, J. du Toit, M. R. Caira and C. Sacht, *J. Chem. Soc., Dalton Trans.*, 1994, 785; (*d*) K. R. Koch and S. Bourne, *J. Chem. Soc., Dalton Trans.*, 1993, 2071; (*e*) K. R. Koch, A. Coetzee and Y. Wang, *J. Chem. Soc., Dalton Trans.*, 1999, 1013.
8 K. R. Koch, *Coord. Chem. Rev.*, 2001, **216–217**, 473.
9 M. Matoetoe and K. R. Koch, unpublished results: M. Matoetoe, MSc Thesis, University of Cape Town, 1990.
10 T. Grimmbacher, C. Sacht and K. R. Koch, *Polyhedron*, 1998, **17**, 267.
11 A. Westra, J. D. C. Miller and K. R. Koch, in *Proceedings of the International Solvent Extraction Conference, ISEC-2002*, K. C. Sole, P. M. Cole, J. S. Preston and D. J. Robinson, ed., SAIMM, Johannesburg, 2002, p. 327.
12 I. B. Douglass and F. B. Dains, *J. Am. Chem. Soc.*, 1934, **56**, 719.
13 P. Pregosin, *Coord. Chem. Rev.*, 1982, **44**, 247.
14 Collect data collection software, Nonius B.V., The Netherlands, 1998.
15 Z. Otwinowski and W. Minor, in *Methods in Enzymology, Vol. 276: Macromolecular Crystallography, Part A*, ed., C. W. Carter, Jr. and R. M. Sweet, Academic Press, San Diego, CA, 1997, pp. 307–326.
16 L. J. Barbour, X-SEED, Graphical Interface for the SHELX Program Suite, University of Missouri, CO, USA, 1999.
17 G. M. Sheldrick, SHELXL97, Program for the Refinement of Crystal Structures, University of Göttingen, Germany, 1997.
18 J.-Y. Lallemand, J. Soulie and J.-C. Chottard, *J. Chem. Soc., Chem. Commun.*, 1980, 436.
19 (*a*) K. R. Koch and M. C. Matoetoe, *Magn. Reson. Chem.*, 1991, **29**, 1158; (*b*) Unpublished results: J. D. C. Miller, PhD Thesis, University of Cape Town, 2000.
20 R. G. Pearson, *J. Am. Chem. Soc.*, 1963, **85**, 3533.
21 D. Argyropoulos, E. Hoffmann, S. Mtongana and K. R. Koch, *Magn. Reson. Chem.*, 2003, **41**, in press.
22 W. Bensch and M. Schuster, *Z. Anorg. Allg. Chem.*, 1992, **615**, 93.
23 L. R. Snyder, J. J. Kirkland and J. L. Glajch, *Practical HPLC Method Development*, John Wiley & Sons Inc., New York, 1997.